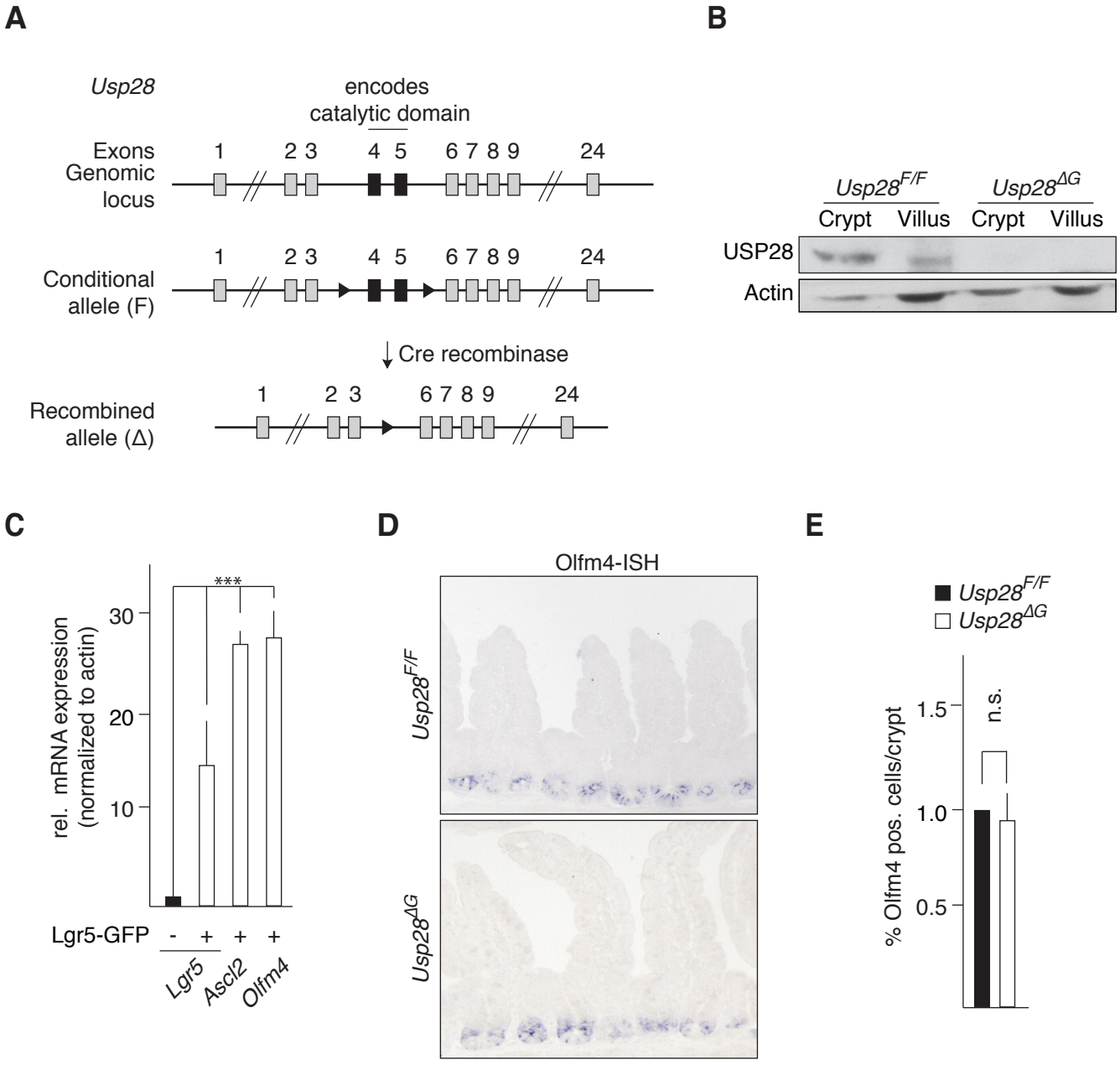

Supplementary Figure 1 (**A**) Gene targeting strategy to generate conditional *Usp28*$^{\Delta}$ animals. Two loxP sites (arrowheads) flank exons 4 and 5 of *Usp28* (*Usp28*^{F}), which encode the catalytic domain. Upon Cre-recombinase activation, exons 4 and 5 are recombined, resulting in a frameshift and the generation of a premature stop-codon (*Usp28*$^{\Delta}$). (**B**) USP28 expression is enhanced in the crypt compared with the villus fraction of the intestine when tissue extracts are analyzed by western blotting. *Usp28*$^{F/F}$; *Villin-Cre* (*Usp28*$^{\Delta G}$) animals show no immunoreactivity against USP28. (**C**) Lgr5-GFP-positive cells also express the stem cell markers Ascl2 and Olfm4 by qPCR. (**D**) In situ hybridisation showing similar Olfm4 staining in *Usp28*$^{\Delta G}$ and control *Usp28*$^{F/F}$animals. (**E**) Quantification of staining in (D).

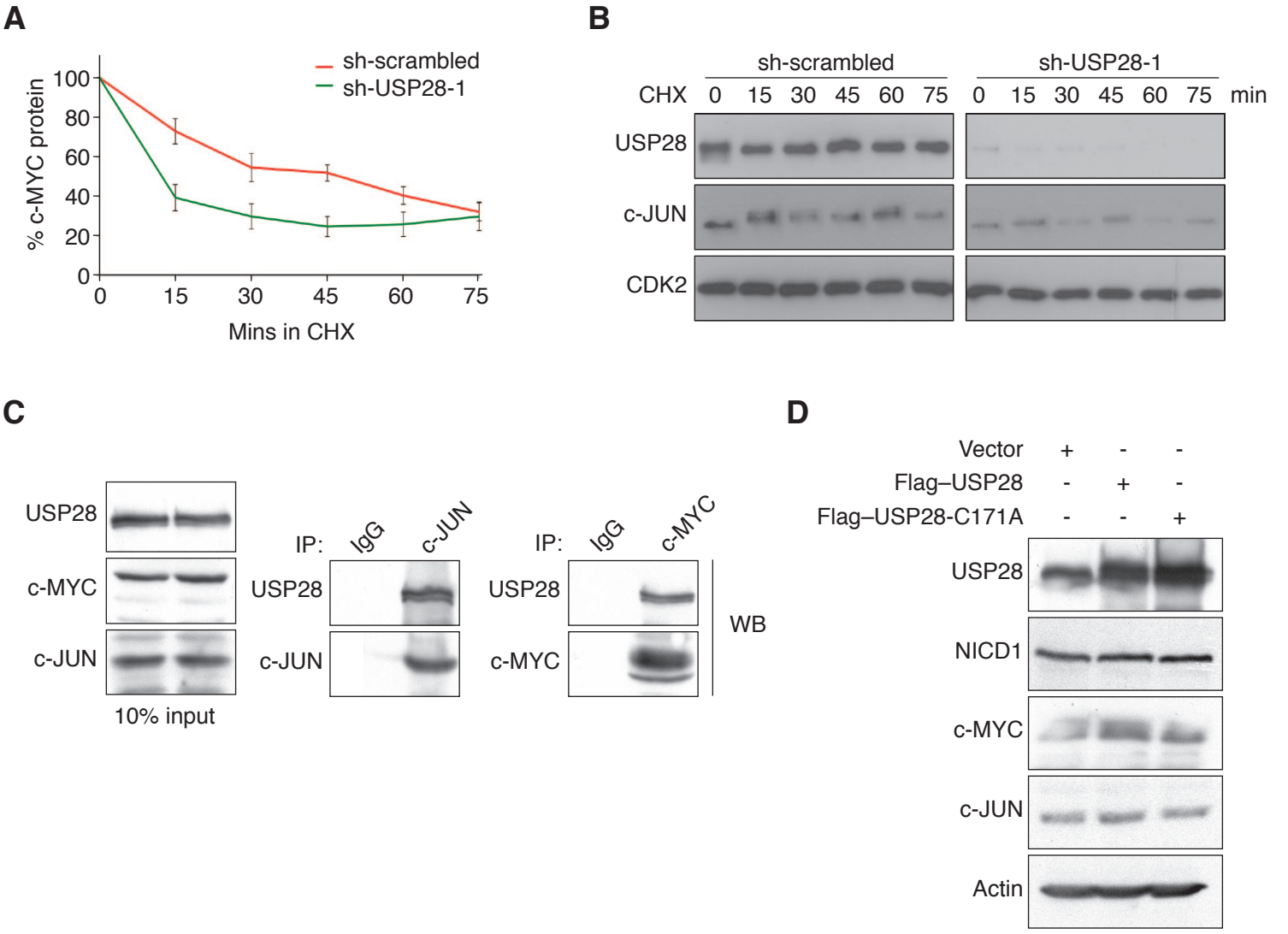

Supplementary Figure 2.
(**A**) Quantification of c-MYC levels over cycloheximide (CHX) time course shown in Fig. 3B. (**B**) Time course of CHX treatment of HCT116 cells transiently transfected with scrambled control shRNA or shRNA targeting USP28. Protein stability of c-JUN was analyzed at the indicated times by western blot. CDK2 is shown as control. (**C**) Endogenous c-JUN and c-MYC co-immunoprecipitate USP28. (**D**) Overexpression of USP28 increases the level of c-MYC and to a lesser extent c-JUN protein. Catalytically impaired C171A mutant USP28 is shown as control.

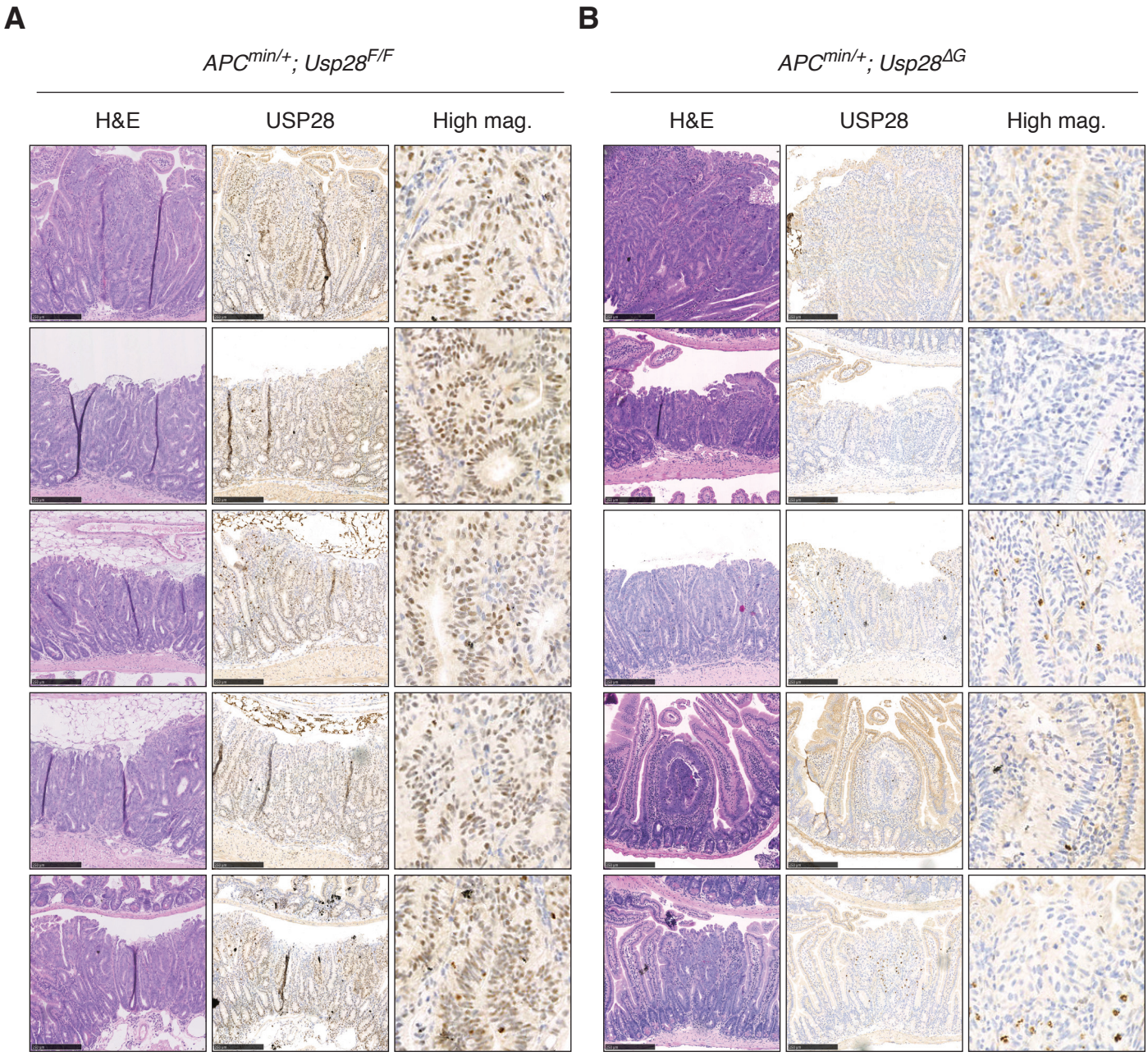

Supplementary Figure 3. Efficient USP28 inactivation in *APC$^{min/+}$; Usp28$^{\Delta G}$* tumours
(A) H&E and USP28 stain of control *APC$^{min/+}$; Usp28$^{F/F}$* tumors. Scale bar = 250µm.
(B) H&E and USP28 stain of *APC$^{min/+}$; Usp28$^{\Delta G}$* tumors. Scale bar = 250µm.

A

Tumor incidence	Lung	Liver	Pancreas	Kidney	Brain	Intestine
APC$^{min/+}$; *Usp28*$^{F/F}$ (n = 22)	0	0	0	0	0	22
APC$^{min/+}$; *Usp28*$^{\Delta G}$ (n = 14)	0	0	0	0	0	14

B

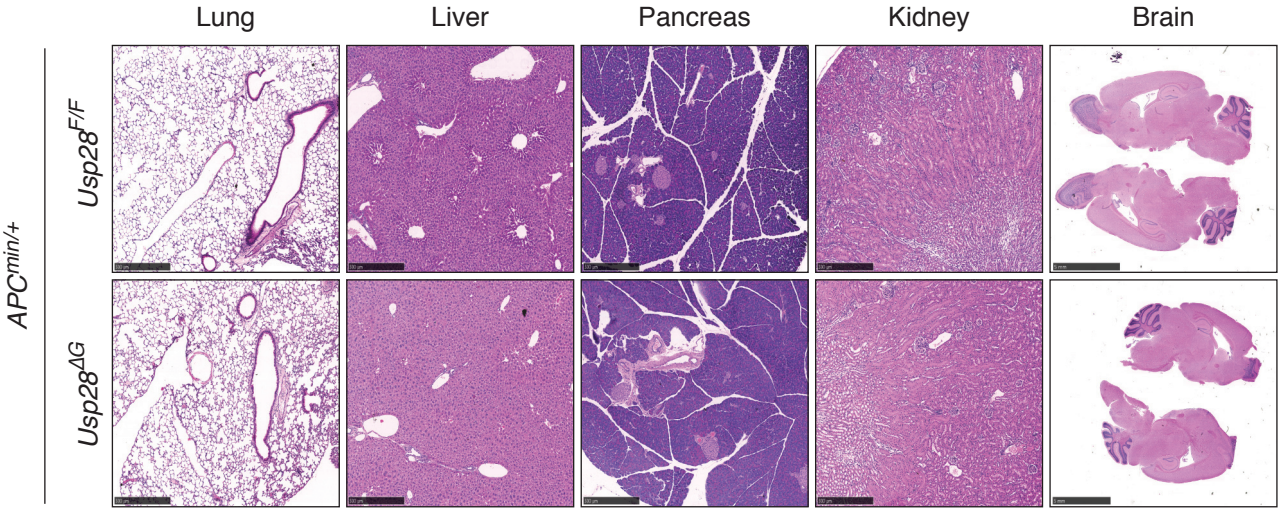

C

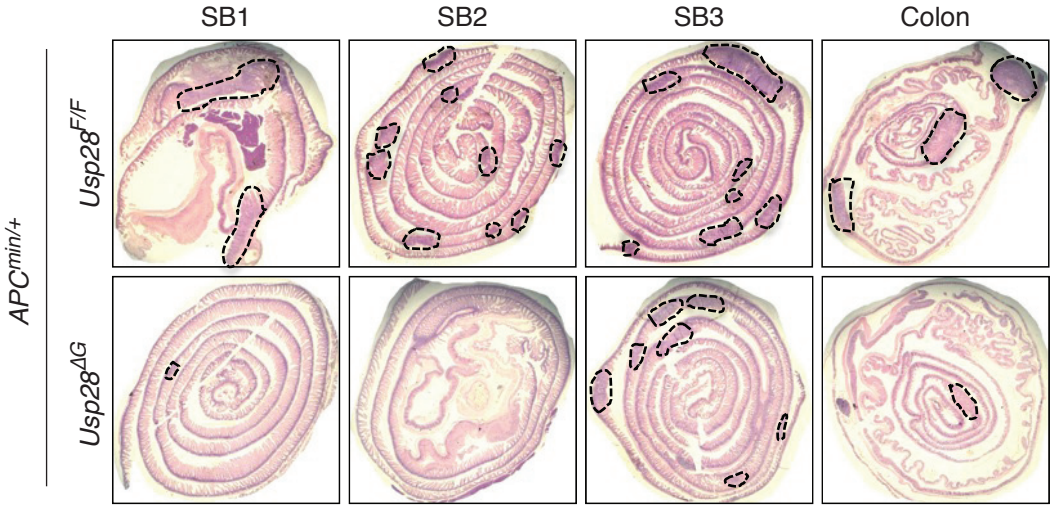

Supplementary Figure 4. *APC*$^{min/+}$; *Usp28*$^{\Delta G}$ animals eventually die of intestinal tumors
(**A**) Tumor incidence in different organs in *Usp28*$^{\Delta G}$ and control animals. (**B**) Sections of different organs stained with H&E. Scale bar = 500µm, except for brain, 5mm. (**C**) Gut rolls showing gross tumor load in small bowel regions 1-3 (SB1-3) and colon.

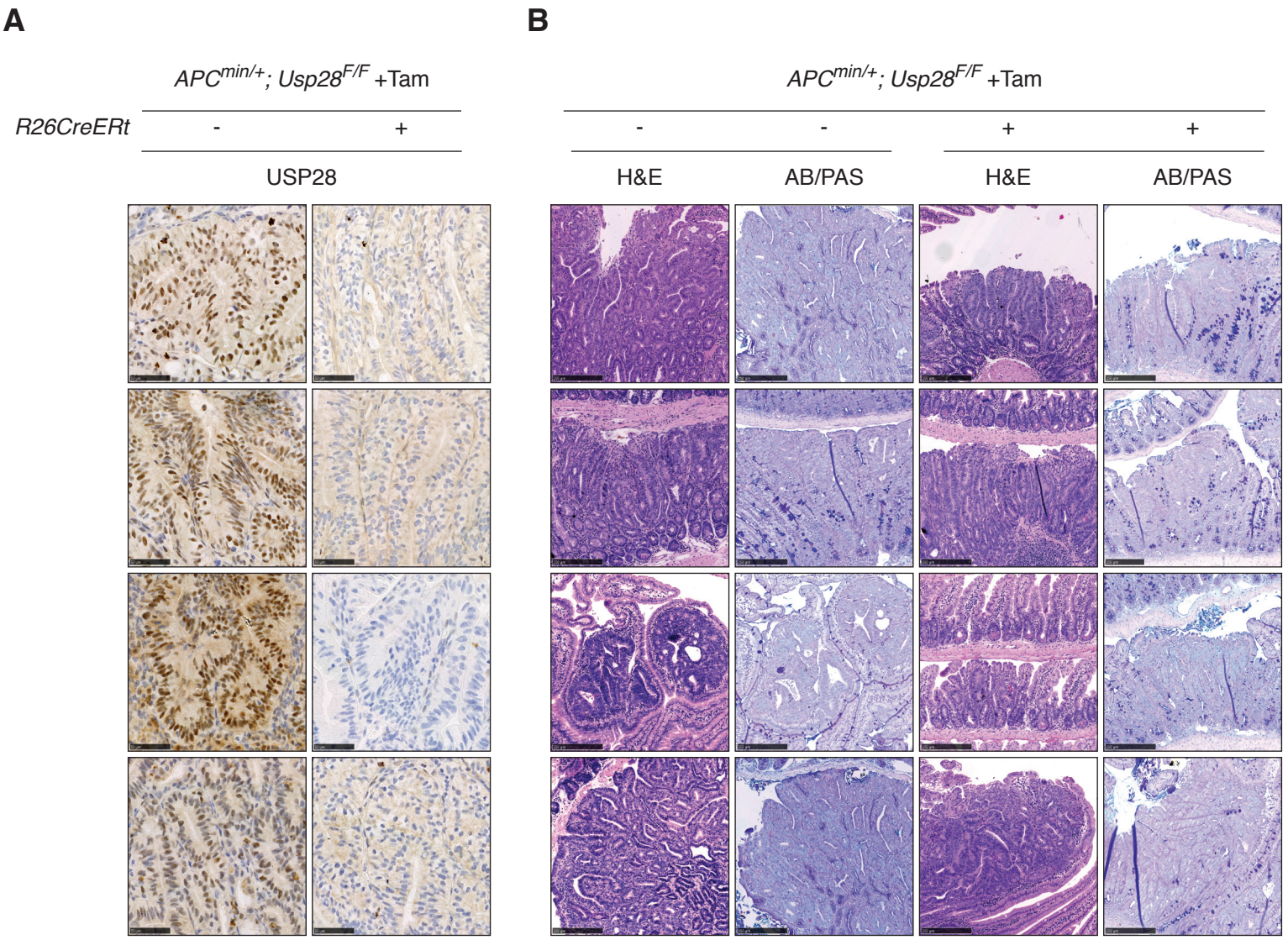

Supplementary Figure 5. USP28 and AB/PAS staining at endpoint in *APC$^{min/+}$; Usp28$^{F/F}$; Rosa26CreERt* mice
(A) USP28 staining shows no reactivation of Usp28 expression in *APC$^{min/+}$; Usp28$^{F/F}$; Rosa26CreERt* tumours. Scale bar = 50µm.
(B) H&E and AB/PAS staining shows increased goblet cell numbers in *APC$^{min/+}$; Usp28$^{F/F}$; Rosa26CreERt* tumours. Scale bar = 250µm.

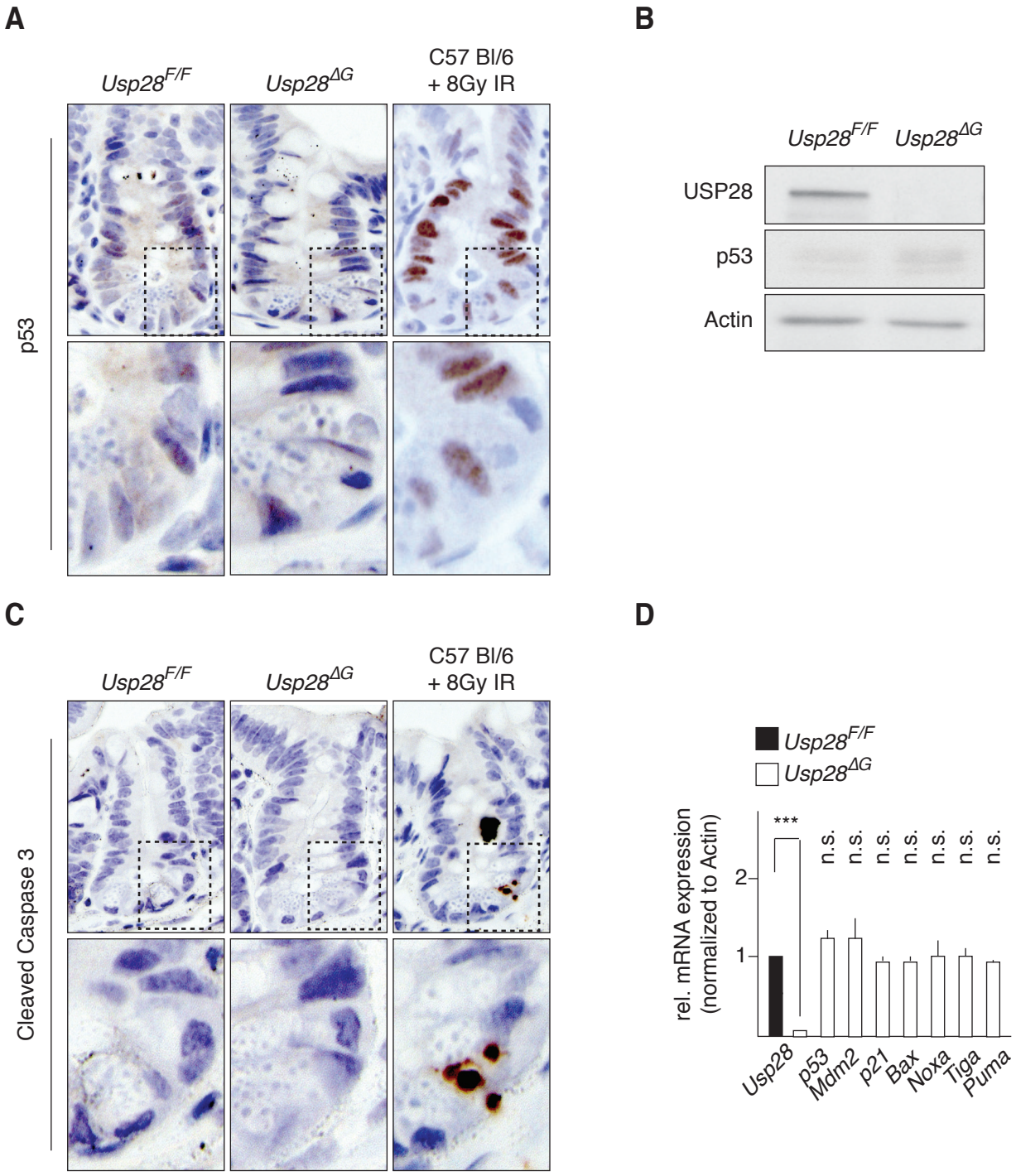

Supplementary Figure 6. p53 and DNA damage response are not active in *Usp28$^{\Delta G}$* intestines
(A) *Usp28$^{F/F}$* and *Usp28$^{\Delta G}$* crypts stained for p53. C57 Bl/6 mouse subjected to 8Gy IR is shown as positive control. Dotted lines indicate area of high magnification (lower row).
(B) *Usp28$^{\Delta G}$* crypt cells show no obvious change in p53 protein levels, as measured by Western blot.
(C) *Usp28$^{F/F}$* and *Usp28$^{\Delta G}$* crypts stained for cleaved caspase 3. C57 Bl/6 mouse subjected to 8Gy IR is shown as positive control. Dotted lines indicate area of high magnification (lower row).
(D) qPCR showing no change in the expression of p53 target genes in *Usp28$^{F/F}$* and *Usp28$^{\Delta G}$* crypts.